M-Channel Linear Phase Perfect Reconstruction Filter Bank With Rational Coefficients

Trac D. Tran, *Member, IEEE*

***Abstract*—This paper introduces a general class of M-channel linear phase perfect reconstruction filter banks (FBs) with rational coefficients. A subset of the presented solutions has dyadic coefficients, leading to multiplierless implementations suitable for low-power mobile computing. All of these FBs are constructed from a lattice structure that is VLSI-friendly, employs the minimum number of delay elements, and robustly enforces both linear phase and perfect reconstruction property. The lattice coefficients are parameterized as a series of zero-order lifting steps, providing fast, efficient, in-place computation of the subband coefficients. Despite the tight rational or integer constraint, image coding experiments show that these novel FBs are very competitive with current popular transforms such as the 8×8 discrete cosine transform and the wavelet transform with 9/7-tap biorthogonal irrational-coefficient filters.**

***Index Terms*—Compression, dyadic coefficients, linear phase filter bank, multiplierless, rational coefficients.**

I. Introduction

MULTIRATE filter banks (FBs) have found tremendous applications in the analysis, processing, and efficient representation of digital signals [1]–[4]. Signal representations by subband samples are usually more compact, more efficient, yet as informative as the time-domain counterparts. Taking advantage of the normally sparse subband sample matrix, we can often obtain significant data compression.

One particular class of FBs that have attracted a lot of recent interests is FBs with integer coefficients [5]–[12]. First of all, integer-coefficient FBs eliminate the truncation error in finite-precision implementations. More importantly, integer-arithmetic implementations in hardware are faster, require less chip area, and consume less power. Thirdly, many integer-coefficient FBs also have very fast multiplierless implementation with simple shift-and-add operations only. Hence, integer FBs are desirable in applications with high data rates as well as in portable computing and wireless communication applications. Integer FBs or integer approximations are already popular in practice. For example, current international image and video compression standards JPEG and MPEG employ several integer approximations of the 8-point discrete cosine transform (DCT) which can be viewed as an irrational-coefficient 8-channel 8-tap linear phase orthogonal FB [13], [14]. The future image compression standard JPEG2000 also utilizes several biorthogonal integer-coefficient wavelet pairs for fast coding/decoding and for lossless compression [15], [16].

This paper introduces a large family of FIR linear phase perfect reconstruction FBs with rational coefficients and good energy compaction property. Integer implementations can be easily found via a common scaling factor. A tighter constraint yields solutions with dyadic coefficients, which lead to efficient multiplierless implementations. Our focus is on the construction of the polyphase matrices as cascades of low-order modular components. Desirable properties such as symmetry, FIR, and perfect invertibility, are propagated by imposing them structurally onto each cascaded module.

A. Outline

The outline of the paper is as follows. In Section II, we offer a review of important background materials, concepts, motivations, and previous related works in multirate FB design using lattice and ladder structures. The next section introduces a general parameterization of polyphase matrices based on lifting steps (also known as ladder structures) and the subset of solutions that allows the construction of M-band rational- and dyadic-coefficient FBs. Parts of Sections II and III are meant to serve as tutorial materials. Design issues and various design examples are presented and discussed in Section IV. The successful application of the newly found family of FBs in image coding is illustrated in Section V. Finally, Section VI ends the paper with a brief summary.

B. Notations

Let $\mathcal{R}$, $\mathcal{Q}$, and $\mathcal{Z}$ denote the sets of real numbers, rational numbers, and integers, respectively. Also, let $\mathcal{D}$ denote the set of dyadic rationals, i.e., all rational numbers that can be represented in the form of $k/2^m$ where $k, m \in \mathcal{Z}$. Bold-faced lower case characters are used to denote vectors while bold-faced upper case characters are used to denote matrices. $\mathbf{A}^T$, $\mathbf{A}^{-1}$, $|\mathbf{A}|$, and a_{ij} denote, respectively, the transpose, the inverse, the determinant, and the ith jth element of the matrix $\mathbf{A}$. When the size of a matrix or vector is not clear from context, capital subscripts will be included. The notation $\mathbf{A} \in \mathcal{Q}^{M \times N}$ or $\mathcal{D}^{M \times N}$ indicates that every element of the $M \times N$ matrix $\mathbf{A}$ is either rational or dyadic, i.e., $a_{ij} \in \mathcal{Q}$ or $a_{ij} \in \mathcal{D}, \forall i, j$.

Several special matrices with reserved symbols are: the polyphase matrix of the analysis bank $\mathbf{E}(z)$, the polyphase matrix of the synthesis bank $\mathbf{R}(z)$, the identity matrix $\mathbf{I}$, the

Manuscript received April 23, 2001; revised December 21, 2001. This work has been supported in part by the National Science Foundation under Grant CCR-0093262 and in part by FastVDO Inc. This paper was presented in part at the SPIE Wavelets Applications in Signal and Image Processing Conference, Denver, CO, July 1999. This paper was recommended by Associate Editor P. P. Vaidyanathan.

The author is with the Department of Electrical and Computer Engineering, The Johns Hopkins University, Baltimore, MD 21218 USA (e-mail: trac@jhu.edu).

Publisher Item Identifier 10.1109/TCSI.2002.800467.

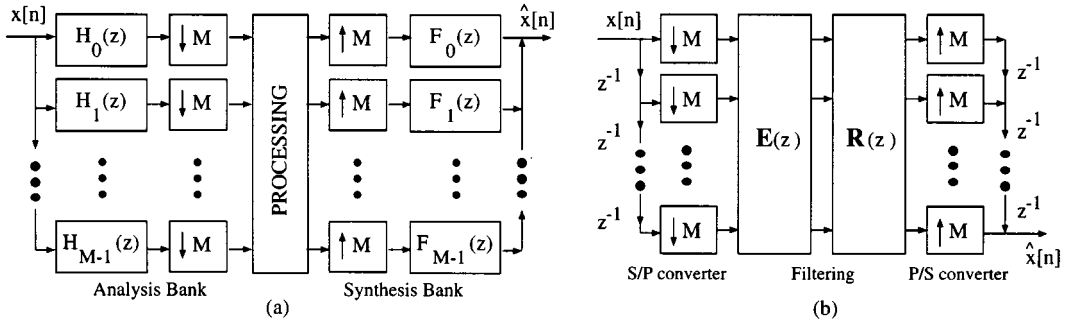

Fig. 1. M-channel uniform FB. (a) Conventional representation. (b) Polyphase representation.

reversal or anti-diagonal matrix $\mathbf{J}$, the null matrix $\mathbf{0}$, a permutation matrix $\mathbf{P}$, and the diagonal matrix $\mathbf{D}$. M and L are usually reserved for the number of channels and the filter length. In this paper, we only consider the class of FBs whose filters all have the same length $L = KM, K \in \mathcal{Z}^+$. An M-channel L-tap FB is sometimes denoted as an $M \times L$ transform. The symbols $h_i[n]$, $H_i(z)$, and $H_i(e^{j\omega}), 0 \le i \le M-1$, stand for the ith analysis filter's impulse response, its associated z-transform, and its Fourier transform. Similarly, the ith synthesis filter is denoted by $f_i[n]$, $F_i(z)$, or $F_i(e^{j\omega})$. For abbreviations, we often use LP, PR, and FB to denote *linear phase*, *perfect reconstruction*, and *FB*.

II. Background and Motivation

A. FB Fundamentals

In this paper, we shall limit the discussions on discrete-time maximally decimated M-channel uniform FBs as depicted in Fig. 1. At the analysis stage, the input signal $x[n]$ is passed through a bank of M analysis filters $H_i(z)$, each of which preserves a frequency band. The overall sampling rate is preserved by the M-fold downsamplers. At the synthesis stage, the subbands are combined by a set of upsamplers and M synthesis filters $F_i(z)$ to form the reconstructed signal $\hat{x}[n]$.

The FB in Fig. 1(a) can also be represented in terms of its polyphase matrices as shown in Fig. 1(b). Here, $\mathbf{E}(z)$ is the analysis bank's polyphase matrix and $\mathbf{R}(z)$ is the synthesis bank's polyphase matrix. Note that both $\mathbf{E}(z)$ and $\mathbf{R}(z)$ are $M \times M$ matrices whose elements are polynomials in z^{-1} [1]. The delay chain and the M-fold downsamplers act as a serial-to-parallel converter. Similarly, in the synthesis bank, the M-fold upsamplers and the delay chain act as a parallel-to-serial converter.

The polyphase representation usually leads to faster and more efficient implementations. It is also very helpful in the FB design process. If $\mathbf{E}(z)$ is invertible with monomial determinant, i.e., $|\mathbf{E}(z)| = z^{-n}, n \in \mathcal{Z}$, one can obtain the output $\hat{x}[n]$ as a pure delayed version of the input $x[n]$, $\hat{x}[n] = x[n - n_0]$, with FIR synthesis filters by simply choosing $\mathbf{R}(z) = \mathbf{E}^{-1}(z)$ [1]–[3]. We call this class of polyphase matrices *FIR invertible*. The resulting FIR FB is said to be *biorthogonal* or to have *perfect reconstruction*. In the case when $\mathbf{R}(z) = \mathbf{E}^{-1}(z) = \mathbf{E}^T(z^{-1})$, the FB is called *paraunitary*.

In numerous practical applications, especially in image and video processing, it is often desired that all analysis and synthesis filters have linear phase (their impulse responses are either symmetric or antisymmetric if the filters have real coefficients). Besides the elimination of the phase distortion, linear phase systems allow us to use simple symmetric extension methods to accurately handle the boundaries of finite-length signals. Furthermore, the linear phase property can be exploited, leading to faster and more efficient FB implementation. If all filters have the same length $L = KM$, it has been well established that the polyphase matrices satisfy the following symmetric property [2] [17]

$$\mathbf{E}(z) = z^{-(K-1)}\mathbf{D}\,\mathbf{E}(z^{-1})\mathbf{J} \quad \text{(analysis)} \tag{1}$$

$$\mathbf{R}(z) = z^{-(K-1)}\mathbf{J}\,\mathbf{R}(z^{-1})\mathbf{D} \quad \text{(synthesis)} \tag{2}$$

where $\mathbf{D}$ is the diagonal matrix with entries being $+1$ or -1 depending on the corresponding filter being symmetric or antisymmetric.

The highly complex problem of designing an M-band FIR linear phase perfect reconstruction FB can be reduced to choosing appropriate polynomial matrices $\mathbf{E}(z)$ and $\mathbf{R}(z)$ such that both FIR invertibility and linear phase condition are satisfied. Additional constraints that yield rational- or dyadic-coefficient filters will be imposed on top. Knowing $\mathbf{E}(z)$ and $\mathbf{R}(z)$, we can easily find the filters $h_i[n]$, $f_i[n]$ and vice versa. This is the approach that will be taken throughout this paper.

B. The Lattice Structure

The lattice structure is one of the most effective and elegant tools in M-channel FB design and implementation. This approach bases on various factorizations of the polyphase matrices $\mathbf{E}(z)$ and $\mathbf{R}(z)$ [17]–[23]. From another viewpoint, in the lattice approach, the polyphase matrix $\mathbf{E}(z)$ or $\mathbf{R}(z)$ is constructed from a cascade of modular low-ordered structures that propagate certain desirable properties (such as linear phase and perfect reconstruction). The lattice structure has been known to offer a fast FB implementation with the minimal number of delay elements, and it can retain all desirable properties regardless of lattice coefficient quantization [1]–[4].

The general M-band linear-phase lattice structure is presented below [21]. The polyphase matrix $\mathbf{E}(z)$ can be factored as

$$\mathbf{E}(z) = \mathbf{G}_{K-1}(z)\mathbf{G}_{K-2}(z)\cdots\mathbf{G}_1(z)\mathbf{G}_0 \tag{3}$$

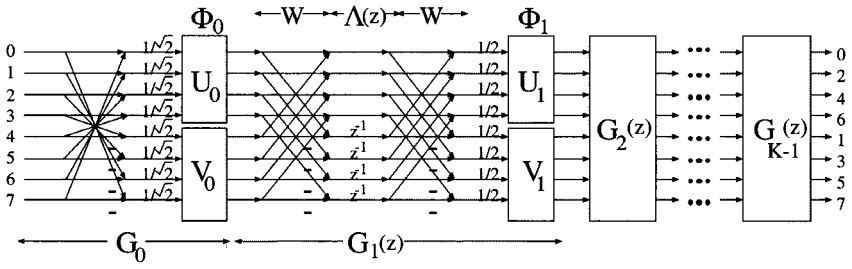

Fig. 2. General lattice structure for M-channel LPPRFB with filter length $L = KM$ (drawn for $M = 8$).

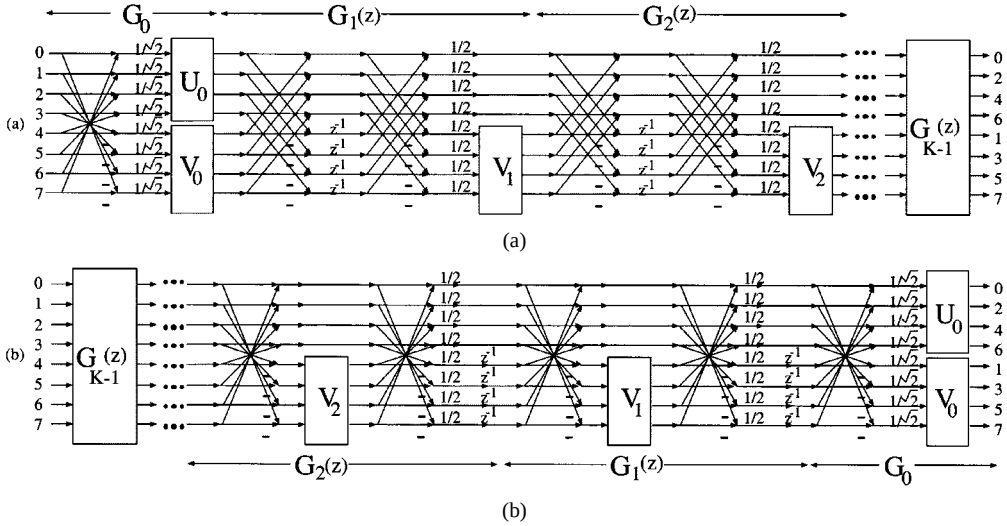

Fig. 3. Simplified lattice structure for M-channel LPPRFB with filter length $L = KM$. (a) Type-I structure. (b) Type-II structure.

where

$$\mathbf{G}_i(z) = \frac{1}{2}\begin{bmatrix}\mathbf{U}_i & \mathbf{0}\\ \mathbf{0} & \mathbf{V}_i\end{bmatrix}\begin{bmatrix}\mathbf{I} & \mathbf{I}\\ \mathbf{I} & -\mathbf{I}\end{bmatrix}\begin{bmatrix}\mathbf{I} & \mathbf{0}\\ \mathbf{0} & z^{-1}\mathbf{I}\end{bmatrix}\begin{bmatrix}\mathbf{I} & \mathbf{I}\\ \mathbf{I} & -\mathbf{I}\end{bmatrix} \triangleq \frac{1}{2}\mathbf{\Phi}_i\mathbf{W}\mathbf{\Lambda}(z)\mathbf{W}, \quad 0 \le i \le K-1 \tag{4}$$

and

$$\mathbf{G}_0 = \frac{1}{\sqrt{2}}\begin{bmatrix}\mathbf{U}_0 & \mathbf{U}_0\mathbf{J}\\ \mathbf{V}_0\mathbf{J} & -\mathbf{V}_0\end{bmatrix} = \frac{1}{\sqrt{2}}\begin{bmatrix}\mathbf{U}_0 & \mathbf{0}\\ \mathbf{0} & \mathbf{V}_0\end{bmatrix}\begin{bmatrix}\mathbf{I} & \mathbf{J}\\ \mathbf{J} & -\mathbf{I}\end{bmatrix} \triangleq \frac{1}{2}\mathbf{\Phi}_0\hat{\mathbf{W}}. \tag{5}$$

This lattice generates even-channel linear phase perfect reconstruction FBs where every filters having the same length $L = KM$ [21]. K is often called the overlapping factor because of the FB connection to lapped transforms [18], [19]. The factorization in (3) is also minimal. The resulting lattice structure employs the fewest number of delays in its implementation — the polyphase matrix can be implemented using no more than $M(K-1)/2$ delay elements. Each cascading structure $\mathbf{G}_i(z)$ increases the filter length by M. All $\mathbf{U}_i$ and $\mathbf{V}_i$, $i = 0, 1, \ldots, K-1$, are arbitrary $M/2 \times M/2$ invertible matrices. The general lattice of the analysis bank is depicted in Fig. 2. The synthesis bank can be obtained by inverting each analysis component one by one.

Following the approach in [22], [23], the structure in Fig. 2 can be simplified significantly since any matrix $\mathbf{U}_i$ can be moved across the butterfly matrices $\mathbf{W}$'s and the delay chain $\mathbf{\Lambda}(z)$ to combine with the free matrices of the next stage, $\mathbf{U}_{i-1}$ and $\mathbf{V}_{i-1}$. By repeating this operation, two different simplified structures shown in Fig. 3 can be derived. The number of free parameters and the complexity of the structure have been reduced by almost 50% while the generality of the structure is still retained. All rational-coefficient designs in this paper are constructed from these two structures.

C. The Lifting Scheme or the Ladder Structure

The lifting scheme, also known as the ladder structure, is a special type of lattice structure, a cascading construction using only elementary matrices – identity matrices with one single nonzero off-diagonal element [7], [10]. 2-channel FBs implemented in ladder structures save roughly half of the computational complexity due to the exploitation of the inter-subband relationship between coefficients. It has been proven that any 2×2 polyphase matrix $\mathbf{E}(z)$ with unity determinant can be factored into a cascade of *predict* $P(z)$, *update* $U(z)$ lifting steps, and a diagonal scaling matrix [10]. Besides the speed improvement, the lifting scheme also offers many other advantages: ability to map integers to integers losslessly, simplicity of integer wavelet design, in-place computation, connection to spatial prediction, and capability of incorporating nonlinear filtering.

D. Motivation

Although there have been numerous works on fast rational- and integer-coefficient two-band FBs [5]–[12], similar research on M-band systems is rather limited. There has been substantial evidence that M-band decompositions are more advantageous than

the dyadic wavelet transform in coding applications. The wavelet-based coder that the FBI designed to compress fingerprints actually imitates a 4-band decomposition using the popular 9/7-tap biorthogonal wavelet [24]. On other image types, M-band FBs, M-band wavelets and wavelet packets almost always yield higher coding performances [15], [16], [18], [19], [21], [25]–[28]. Furthermore, M-channel FBs in reverse (the synthesis bank comes first) are also useful in communications as crosstalk-free transmultiplexers [2], [29] and precoders [30], [31].

When $M > 2$, there is no simple spectral factorization method which has worked well in 2-channel FB design. One has to rely on other approaches such as lattice structure parameterization, time-domain optimization, and cosine modulation [1]–[4]. Even in the 2-channel case, the lifting scheme is predominantly used for fast implementation rather than for FB design. It is unclear how to generalize the lifting result to build an entire class of M-band FBs with many desired properties such as linear-phase and integer-coefficient. In the next section, we present rational- and integer-coefficient building blocks that can be employed to construct fast integer (even multiplierless) FBs with an arbitrary number of channels.

III. Rational- and Integer-Coefficient Structures

A. Problem Formulation

The FBs of interest in this paper all satisfy the definition below.

Definition 1: An M-channel FB is said to have rational coefficients if every analysis as well as synthesis filter coefficient is rational, i.e., $h_i[n], f_i[n] \in \mathcal{Q}, \forall n \in \mathcal{Z}$ and $\forall i \in \{0,1,\ldots,M-1\}$. An M-channel FB is said to have integer (or dyadic) coefficients if every analysis as well as synthesis filter coefficient is dyadic, i.e., $h_i[n], f_i[n] \in \mathcal{D}, \forall n \in \mathcal{Z}$ and $\forall i \in \{0,1,\ldots, M-1\}$.

Integer implementations can be easily obtained by scaling the rational analysis and synthesis filter coefficients $h_i[n]$ and $f_i[n]$ by their corresponding common denominators C_a and C_s respectively. Perfect reconstruction can be achieved by one scaling factor, $1/C_aC_s$. Preferably, C_a and C_s should be as small as possible so that the dynamic range of the subband samples is limited and the computational complexity is minimized. However, one integer division needs to be spent on each output sample, and perfect integer mapping cannot be guaranteed.

The dyadic subset, $h_i[n], f_i[n] \in \mathcal{D}$, of rational-coefficient FBs has even greater value in practice. In the dyadic case, FBs can be implemented using only addition and binary shifting operations. Hence, these are often called *multiplierless* or *multiplier-free* FBs. In this case, the scaling factor $1/C_aC_s$ is dyadic; hence, the input signal can be recovered perfectly using a binary shift.

From the definition of the polyphase representations [1]

$$H_i(z) = \sum_{\ell=0}^{M-1} z^{-\ell} E_{i\ell}(z^M)$$
$$F_i(z) = \sum_{\ell=0}^{M-1} z^{-(M-1-\ell)} R_{\ell i}(z^M)$$

an equivalence to *Definition 1* above is that every element of both polyphase matrices is a polynomial with rational coefficients. In other words, if the polyphase matrices are represented as $\mathbf{E}(z) = \sum_n \mathbf{E}_n z^{-n}$ and $\mathbf{R}(z) = \sum_n \mathbf{R}_n z^{-n}$, then $\mathbf{E}_n \in \mathcal{Q}^{M\times M}$ and $\mathbf{R}_n \in \mathcal{Q}^{M\times M}, \forall n \in \mathcal{Z}$. Thus, the notations $\mathbf{E}(z) \in \mathcal{Q}^{M\times M}(z)$ and $\mathbf{R}(z) \in \mathcal{Q}^{M\times M}(z)$ are often used to indicate that the resulting FB has rational coefficients.

B. Rational and Dyadic Lifting-Based Cascades

From the simplified lattice structures in Fig. 3, it is clear that the key to rational or dyadic-coefficient solutions hinges on the free-parameter scalar matrices $\mathbf{U}_0$, $\mathbf{V}_i, 0 \le i \le K-1$, and their inverses. Since the fixed components – butterfly matrices $\{\mathbf{W}, \hat{\mathbf{W}}\}$, delay chains $\{\mathbf{\Lambda}(z), \hat{\mathbf{\Lambda}}(z)\}$, and their inverses – are already dyadic components, it is sufficient to impose rational and dyadic property on the free scalar matrices.

One problem arises from the irrational $1/\sqrt{2}$ normalization factors at the initial butterfly stage $\mathbf{G}_0$ of both Type-I and Type-II structure in Fig. 3. There are several simple solutions to this problem. First, for two-dimensional applications, the $1/\sqrt{2}$ factor in the row-wise filtering stage can be delayed and later combined with the $1/\sqrt{2}$ factor in the column-wise filtering stage to form a dyadic scaling factor 1/2. Second, all $1/\sqrt{2}$ factors in $\mathbf{G}_0$ can be deferred and later combined with the $1/\sqrt{2}$ factors in the inverse component $\mathbf{G}_0^{-1}$ of the synthesis bank.

Both of these solutions have a common drawback. They increase the dynamic range of intermediate data and final subband samples. In order to minimize the bit depth and to achieve consistently high performances in a unifying lossless/lossy coding framework, the FB should map integers to integers with limited bit expansion. A solution to the dynamic range problem is to redistribute the $1/\sqrt{2}$ factors to obtain unbalanced, unnormalized $\mathbf{G}_0$ and $\mathbf{G}_0^{-1}$ matrices as follows:

$$\mathbf{G}_0 = \begin{bmatrix} \mathbf{U}_0 & \mathbf{0} \\ \mathbf{0} & \mathbf{V}_0 \end{bmatrix} \begin{bmatrix} \frac{1}{2}\mathbf{I} & \frac{1}{2}\mathbf{J} \\ \mathbf{J} & -\mathbf{I} \end{bmatrix} \tag{6}$$

and

$$\mathbf{G}_0^{-1} = \begin{bmatrix} \mathbf{I} & \frac{1}{2}\mathbf{J} \\ \mathbf{J} & -\frac{1}{2}\mathbf{I} \end{bmatrix} \begin{bmatrix} \mathbf{U}_0^{-1} & \mathbf{0} \\ \mathbf{0} & \mathbf{V}_0^{-1} \end{bmatrix}. \tag{7}$$

This solution is commonly employed in integer wavelet design and implementation [3]. However, the unbalanced nature of the FB makes some subbands have more energy than they should. Hence, in coding applications, the following quantization and entropy coding steps need to be compensated accordingly.

The 1/2 scaling factor in each cascaded structure $\mathbf{G}_i(z)$ can also be redistributed in similar fashion. For example, the type-I structure in Fig. 3(a) can be modified as follows:

$$\mathbf{G}_i(z) = \begin{bmatrix} \mathbf{I} & \mathbf{0} \\ \mathbf{0} & \mathbf{V}_i \end{bmatrix} \begin{bmatrix} \frac{1}{2}\mathbf{I} & \mathbf{I} \\ \frac{1}{2}\mathbf{I} & -\mathbf{I} \end{bmatrix} \begin{bmatrix} \mathbf{I} & \mathbf{0} \\ \mathbf{0} & z^{-1}\mathbf{I} \end{bmatrix} \begin{bmatrix} \mathbf{I} & \mathbf{I} \\ \frac{1}{2}\mathbf{I} & -\frac{1}{2}\mathbf{I} \end{bmatrix}. \tag{8}$$

The resulting structure after taking into account (6)–(8) is illustrated in Fig. 4 where $\mathbf{U}_0$ and $\mathbf{V}_i$ are free scalar invertible matrices. Linear phase and perfect reconstruction are structurally

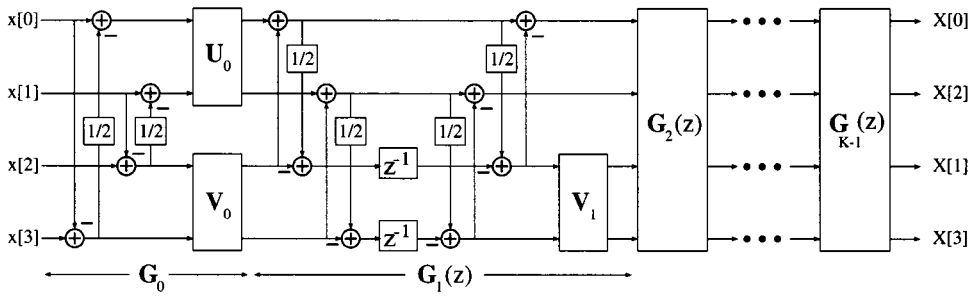

Fig. 4. General construction of fast M-band integer-coefficient FBs (type-I, drawn for $M = 4$).

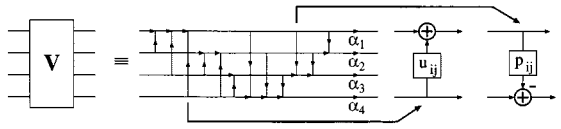

Fig. 5. Parameterization of an invertible matrix as product of lifting steps p_{ij}, u_{ij}, and diagonal scaling factors α_i.

enforced by the lattice. The type-II structure in Fig. 3(b) can also be rewritten accordingly

$$\mathbf{G}_i(z) = \begin{bmatrix} \mathbf{I} & \mathbf{0} \\ \mathbf{0} & z^{-1}\mathbf{I} \end{bmatrix} \begin{bmatrix} \mathbf{I} & \frac{1}{2}\mathbf{J} \\ \mathbf{J} & -\frac{1}{2}\mathbf{I} \end{bmatrix} \begin{bmatrix} \mathbf{I} & \mathbf{0} \\ \mathbf{0} & \mathbf{V}_i \end{bmatrix} \begin{bmatrix} \frac{1}{2}\mathbf{I} & \frac{1}{2}\mathbf{J} \\ \mathbf{J} & -\mathbf{I} \end{bmatrix}. \tag{9}$$

M-band LPPRFBs with rational or dyadic coefficients can be easily constructed if $\{\mathbf{U}_0, \mathbf{V}_i; 0 \le i \le K-1\} \in \mathcal{Q}^{M/2\times M/2}$ or $\{\mathbf{U}_0, \mathbf{U}_0^{-1}, \mathbf{V}_i, \mathbf{V}_i^{-1}; 0 \le i \le K-1\} \in \mathcal{D}^{M/2\times M/2}$, respectively. This topic is the focus of the next section.

C. Matrix Parameterization

As previously mentioned, the set $\{\mathbf{U}_0, \mathbf{V}_i; 0 \le i \le K-1\}$ holds all of the FB's degrees of freedom. The purpose of matrix parameterization is to completely capture this set of invertible matrices using the fewest number of independent parameters. From a design perspective, matrix parameterization provides a powerful FB design tool since the free parameters can be varied independently and arbitrarily without affecting the most desirable FB characteristics. Unconstrained optimization can be performed on the free-parameter space to obtain other features such as high coding gain, regularity, and high stopband attenuation. An efficient parameterization of invertible matrices for integer- and rational-coefficient FB design is based on elementary matrices as depicted in Fig. 5.

Definition 2: An $N \times N$ matrix is called elementary if it is an identity matrix $\mathbf{I}$ with one single nonzero off-diagonal entry. The symbol $\mathbf{U}_{ij}$ will be used when the corresponding nonzero off-diagonal entry u_{ij} is above the diagonal, i.e., $i < j$ where i, j indicate the location of the nonzero off-diagonal element. If the nonzero off-diagonal entry is below the diagonal, i.e., $i > j$, symbols $\mathbf{P}_{ij}$ and p_{ij} will be used instead.

The elementary matrix is often called a *lifting step* in this paper. One characteristic of an elementary matrix is that its inverse is also elementary. Moreover, the inverse simply involves a negation of the nonzero off-diagonal entry p_{ij} or u_{ij}. It is obvious that p_{ij} (or u_{ij}) $\in \mathcal{Q}$ or $\mathcal{D}$ is equivalent to $\mathbf{P}_{ij}$ and $\mathbf{P}_{ij}^{-1}$ (or $\mathbf{U}_{ij}$ and $\mathbf{U}_{ij}^{-1}$) $\in \mathcal{Q}^{N\times N}$ or $\mathcal{D}^{N\times N}$, respectively. This is the key to our rational-coefficient or dyadic-coefficient FB design. The theorem below establishes the parameterization of any invertible matrix using a cascade of elementary, diagonal, and permutation matrices.

Theorem 1: Every $N \times N$ invertible matrix $\mathbf{V}$ can be completely characterized by $N(N-1)$ elementary matrices, N diagonal scaling factors, and a permutation matrix.

This is the LDU matrix factorization and we refer the readers to [32] for a formal proof. Any invertible matrix $\mathbf{V}$ can be written as $\mathbf{V} = \mathbf{PLDU}$ where $\mathbf{P}$ is a permutation matrix, $\mathbf{L}$ is a lower triangular matrix, $\mathbf{D}$ is a diagonal matrix, and $\mathbf{U}$ is an upper triangular matrix. All diagonal entries of both $\mathbf{L}$ and $\mathbf{U}$ are unity. Each of the lower or upper triangular matrix can be factored into $N(N-1)/2$ elementary matrices whose off-diagonal entries are labeled p_{ij} or u_{ij}. The parameters p_{ij} and their corresponding elementary matrices $\mathbf{P}_{ij}$ form the lower-triangular matrix $\mathbf{L}$, i.e., $\mathbf{L} = \prod_{i,j} \mathbf{P}_{ij}$, whereas the parameters u_{ij} and their corresponding elementary matrices $\mathbf{U}_{ij}$ form the upper-triangular matrix $\mathbf{U}$, i.e., $\mathbf{U} = \prod_{i,j} \mathbf{U}_{ij}$. The diagonal scaling factors labeled α_i are contained in the diagonal matrix $\mathbf{D}$ and they hold the key to invertibility. This LU parameterization in FB design first appears in [7] under the name *ladder structure*.

Since the permutation matrix is a simple re-routing, we usually ignore it in the parameterization. The diagonal scaling factors are strategically placed at the end of the structure so that they can be absorbed into the quantization stage whenever possible. This requires a simple modification of the factorization:

$$\mathbf{V} = \mathbf{PLDU} = \mathbf{PDD^{-1}LDU} = \mathbf{PD\hat{L}U}$$

where $\hat{\mathbf{L}} \triangleq \mathbf{D}^{-1}\mathbf{LD}$ is still a lower triangular matrix with unity diagonal elements. The LDU parameterization of any arbitrary invertible matrix $\mathbf{V}$ is illustrated in Fig. 5. The following theorem imposes the rationality condition on $\mathbf{V}$, its inverse $\mathbf{V}^{-1}$, and all filter coefficients.

Theorem 2: If $\{p_{ij}, u_{ij}, \alpha_i\} \in \mathcal{Q}$, then $\{\mathbf{V}, \mathbf{V}^{-1}\} \in \mathcal{Q}^{N\times N}$ and $\{h_i[n], f_i[n]; \forall i, n \in \mathcal{Z}\} \in \mathcal{Q}$.

Proof: First, since $\mathcal{Q}$ is close under addition and multiplication, if $\{p_{ij}, u_{ij}, \alpha_i\} \in \mathcal{Q}$, then $\{\mathbf{P}_{ij}, \mathbf{D}, \mathbf{U}_{ij}\} \in \mathcal{Q}^{N\times N}$, hence $\{\mathbf{L}, \mathbf{D}, \mathbf{U}\} \in \mathcal{Q}^{N\times N}$ and $\mathbf{V} = \mathbf{PLDU} \in \mathcal{Q}^{N\times N}$. Similarly, since the set of parameters that characterizes the inverse $\{-p_{ij}, -u_{ij}, 1/\alpha_i\} \in \mathcal{Q}$, it is easy to establish that $\mathbf{V}^{-1} = \mathbf{U}^{-1}\mathbf{D}^{-1}\mathbf{L}^{-1}\mathbf{P}^{-1} \in \mathcal{Q}^{N\times N}$ as well. Now, consider the cascading modules $\mathbf{G}_0$ in (6) and $\mathbf{G}_i(z)$ in (8) and (9). If $\{\mathbf{U}_0, \mathbf{V}_i; i = 0, 1, \ldots, K-1\} \in \mathcal{Q}^{M/2\times M/2}$, then $\{\mathbf{G}_0, \mathbf{G}_0^{-1}\} \in \mathcal{Q}^{M\times M}$ and $\{\mathbf{G}_i(z), \mathbf{G}_i^{-1}(z); i = 1, 2, \ldots, K-$

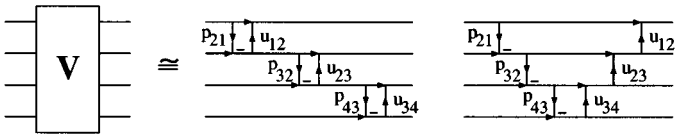

Fig. 6. Simplified parameterization of an invertible matrix.

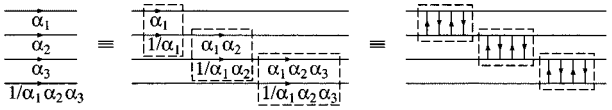

Fig. 7. Example of decomposing diagonal scaling factors into lifting steps. From left to right: original scaling factors; decomposition into $\{K, 1/K\}$ pairing; decomposition into lifting steps.

$1\} \in \mathcal{Q}^{M\times M}(z)$. Hence, for the Type-I lattice as in Fig. 3(a), we have $\mathbf{E}(z) = [\prod_{i=K-1}^{1} \mathbf{G}_i(z)]\mathbf{G}_0 \in \mathcal{Q}^{M\times M}(z)$ and $\mathbf{R}(z) = \mathbf{G}_0^{-1}[\prod_{i=1}^{K-1} \mathbf{G}_i^{-1}(z)] \in \mathcal{Q}^{M\times M}(z)$. For the Type-II lattice as in Fig. 3(b), $\mathbf{E}(z) = \mathbf{G}_0 \prod_{i=1}^{K-1} \mathbf{G}_i(z) \in \mathcal{Q}^{M\times M}(z)$ and $\mathbf{R}(z) = [\prod_{i=K-1}^{1} \mathbf{G}_i^{-1}(z)]\mathbf{G}_0^{-1} \in \mathcal{Q}^{M\times M}(z)$. In other words, $\{h_i[n], f_i[n]; \forall i, n \in \mathcal{Z}\} \in \mathcal{Q}$. ■

Theorem 3: If $\{p_{ij}, u_{ij}\} \in \mathcal{D}$ and $\{\alpha_i\} \in \{2^k; k \in \mathcal{Z}\}$, then $\{h_i[n], f_i[n] \forall i, n \in \mathcal{Z}\} \in \mathcal{D}$.

Proof: This is a straightforward extension of the result in *Theorem 2*. The complication here involves the scaling factors α_i since their inverses are not guaranteed to be dyadic even if they themselves are. We still have $\{\mathbf{L}, \mathbf{U}, \mathbf{L}^{-1}, \mathbf{U}^{-1}\} \in \mathcal{D}^{N\times N}$ if $\{p_{ij}, u_{ij}\} \in \mathcal{D}$. However, $\{\mathbf{D}, \mathbf{D}^{-1}\} \in \mathcal{D}^{N\times N}$ if and only if $\{\alpha_i\} \in \{2^k; k \in \mathcal{Z}\}$. From these conditions, FBs with integer coefficients can be realized by following the same reasoning as in the proof of Theorem 2. The most convenient path to dyadic-coefficient FBs is to set all diagonal scaling factors to unity. ■

Computational Complexity: As each elementary matrix takes one multiplication and one addition, and the diagonal matrix requires N multiplications, the computational complexity of each matrix multiplication is, at most, equal to that of direct multiplication under this parameterization: $N(N-1)+N = N^2$ multiplications and $N(N-1)$ additions. In most cases, the computational complexity can be reduced significantly by setting the diagonal scaling factors to unity, setting many lifting step to zero, or choosing the lifting coefficients to be dyadic as described in the next section. An example of a reduced-complexity parameterization is shown in Fig. 6 where entries close to the diagonal axis are emphasized. The complexity is now reduced to only $2(N-1)$ multiplications and $2(N-1)$ additions.

Lifting Decomposition for Scaling Factors: If we restrict the determinant of $\mathbf{V}$ to ± 1, the N scaling factors α_i in $\mathbf{D}$ can be converted into lifting steps as well, i.e., the entire matrix $\mathbf{V}$ in this case can be represented using only lifting steps.

In the 2×2 case, it is well-known that the diagonal scaling matrix $\begin{bmatrix} K & 0 \\ 0 & 1/K \end{bmatrix}$ can be factored into four lifting steps [10]. In the $N \times N$ case, the product of the diagonal elements α_i is unity. Hence, they can be divided into $N-1$ successive pairs, each with unity product. In other words, since $\prod_{i=1}^{N} \alpha_i = 1$, the following pairings can be obtained:

$$\left\{\alpha_1, \frac{1}{\alpha_1}\right\}, \left\{\alpha_1\alpha_2, \frac{1}{\alpha_1\alpha_2}\right\}, \left\{\alpha_1\alpha_2\alpha_3, \frac{1}{\alpha_1\alpha_2\alpha_3}\right\}, \ldots, \left\{\prod_{i=1}^{N-1} \alpha_i, \frac{1}{\prod_{i=1}^{N-1} \alpha_i}\right\}$$

as demonstrated in Fig. 7. Each pair can then be factored into a cascade of four lifting steps. However, many of these scaling factors typically can be folded into the quantization stepsizes of the encoder. That is why we choose to place them at the end of the factorization in Fig. 5.

Dyadic Lifting Steps and Multiplierless Construction: One advantage that the lifting scheme offers is the versatility and the simplicity in constructing fast transforms that can map integers to integers as illustrated in Fig. 8. If a *floor* (or *round*, or *ceiling*) operator is placed in each lifting step, the FB can now map integers to integers with perfect reconstruction regardless of the lifting step has integer coefficients or not. Moreover, if the lifting step is chosen to be dyadic, the nonlinear operation can be incorporated into the division using binary bit shift. A scalar lifting step of value $k/2^m$ can be implemented as a multiplication by k followed by a division by $1/2^m$. Division by $1/2^m$ followed by a truncation is equivalent to a binary shift by m places. The numerator k can be easily implemented using bit shift and add operations, or we can split the fraction $k/2^m$ into a cascade of pure power-of-two lifting steps, i.e., $k/2^m = \sum_i 1/2^i$. The latter approach leads to an implementation with solely binary right-shifts, preventing the bit-depth expansion in intermediate results. With all scaling factors set to unity, multiplierless FBs can be easily constructed using this method. If the scaling factors α_i are powers of two, we can still retain the multiplierless feature on both banks.

With all free-parameter matrices $\mathbf{U}_0$ and $\mathbf{V}_i$ constructed from dyadic lifting steps, the structure in Fig. 3 or Fig. 4 is very regular and modular: the same shift-and-add module is employed repeatedly. This is very desirable in practical VLSI implementation where irregularity often translates to awkward transistor placements, leading to larger chip area and power consumption [33]. The challenge is how to choose the minimal set of lifting steps that yield optimal or near-optimal coding performances. We shall demonstrate in Section IV via many design examples that not all lifting steps are needed and most, if not all, diagonal scaling factors can be set to unity without having to sacrifice much coding performances.

IV. Design

The FB structure presented in the previous section already has high practical value: FIR, linear phase, and perfect reconstruction regardless of the choices of the lifting $\{p_{ij}, u_{ij}\}$ and scaling $\{\alpha_i\}$ parameters. Restricting these parameters to rationals yields rational-coefficient FBs. However, to achieve high coding performance in practice, several other properties such as coding gain and regularity are also needed. Practical FBs based on our structure can be obtained using two methods: approximation and optimization.

A. Approximation

In the approximation approach, one can study closely existing high-performance FBs and try to replace their floating-point

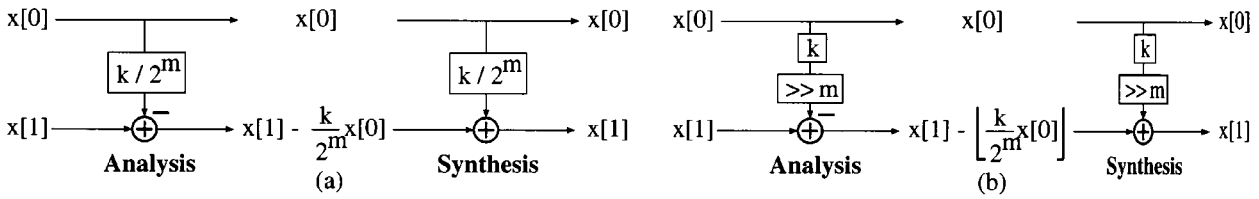

Fig. 8. Example of a lifting step and its implementations. (a) Original lifting step. (b) Approximation that can map integers to integers, using only shift-and-add operations.

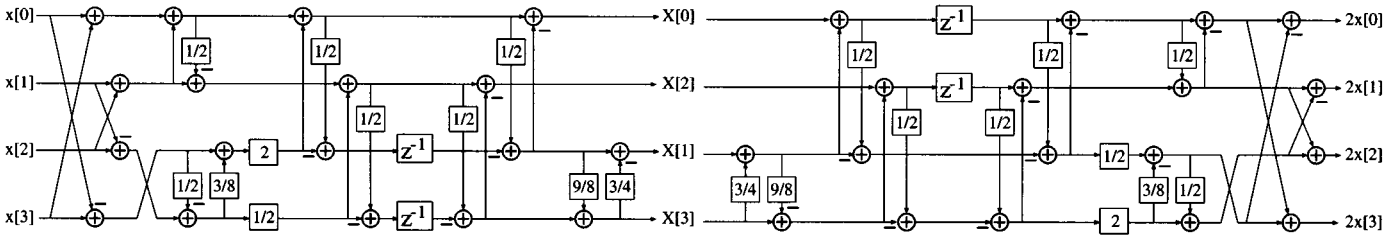

Fig. 9. Design Example 1: 4-channel 8-tap integer LPPRFB. Left: analysis bank. Right: synthesis bank.

components by rational or integer components. One typical example is the systematic approximation of the popular rotation angle, the basic building block of many FBs in the current literature such as the DCT [34], the LOT [18], and its generalized version GenLOT [19].

A plane rotation can be represented using three lifting steps or two lifting steps and two scaling factors as follows [10]:

$$\begin{bmatrix} c_i & s_i \\ -s_i & c_i \end{bmatrix} = \begin{bmatrix} 1 & -\frac{c_i-1}{s_i} \\ 0 & 1 \end{bmatrix} \begin{bmatrix} 1 & 0 \\ -s_i & 1 \end{bmatrix} \begin{bmatrix} 1 & -\frac{c_i-1}{s_i} \\ 0 & 1 \end{bmatrix} = \begin{bmatrix} c_i & 0 \\ 0 & \frac{1}{c_i} \end{bmatrix} \begin{bmatrix} 1 & 0 \\ -s_i c_i & 1 \end{bmatrix} \begin{bmatrix} 1 & t_i \\ 0 & 1 \end{bmatrix}$$

where $c_i \triangleq \cos\theta_i$, $s_i \triangleq \sin\theta_i$, and $t_i \triangleq \tan\theta_i$. Therefore, we can simply try to replace each plane rotation approximately by rational-coefficient ladder structures. The most straightforward method is to obtain the irrational lifting coefficients $\{((c_i-1)/s_i), s_i, s_i c_i, t_i\}$, and then replace them by rational or dyadic values, for example, truncating the binary representations of these parameters.

B. Optimization

The other design approach is to employ an unconstrained nonlinear optimization where certain FB desirable properties such as coding gain and regularity are maximized.

Coding Gain: The coding gain of a FB is defined as the reduction in transform coding mean-square error over pulse-code modulation (PCM) which simply quantizes the samples of the signal with the desired number of bits per sample. Define σ_x^2 as the variance of the input signal $x[n]$, $\sigma_{x_i}^2$ as the variance of the ith subband, and $||f_i||^2$ as the $\mathcal{L}^2$ norm of the ith synthesis filter. With several assumptions including scalar quantization and a sufficient large bit rate, the generalized coding gain can be formulated as [35]

$$C_{\text{coding gain}} = 10\log_{10} \frac{\sigma_x^2}{\left(\prod_{i=0}^{M-1} \sigma_{x_i}^2 ||f_i||^2\right)^{1/M}}. \qquad (10)$$

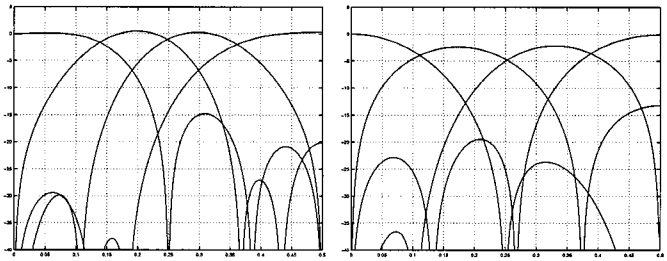

Fig. 10. Normalized frequency responses of the 4-channel 8-tap integer LPPRFB in Design Example 1. Left: analysis bank. Right: synthesis bank.

The signal $x[n]$ is the commonly-used AR (1) process with intersample autocorrelation coefficient $\rho = 0.95$. The coding gain can be thought of as an approximate measure of the FBs energy compaction capability. Among the listed criteria, higher coding gain correlates most consistently with higher objective performance (measured in MSE or PSNR). FBs with higher coding gain compact more signal energy into a fewer number of coefficients, and this leads to more efficient entropy coding.

Regularity: A recursive cascade of most of the previously mentioned M-channel FBs on the lowpass channel output can generate M-band wavelets. Smoothness of the continuous-time *scaling function* $\phi(t)$ and *wavelet function* $\psi(t)$ which result from infinite iteration of the FB's lowpass channel is crucial in signal approximation and interpolation. The smoothness of $\phi(t)$, also termed *regularity*, correlates closely to the number of zeroes at aliasing frequencies $\omega = 2k\pi/M, k = 1, 2, \ldots, M-1$ of the lowpass filters $H_0(z)$ and $F_0(z)$ [25]. These zeroes are also called *vanishing moments* since a linear combination of the corresponding scaling function and its time-shifted versions can represent any piecewise polynomial of degree $K-1$ where K is the degree of regularity (the number of zeros at aliasing frequencies).

In traditional 2-band wavelets, all of the system's degrees of freedom are allocated to these vanishing moments, or zeros at π. The compact-support filters are easily obtained from the spectral factorization of the maxflat halfband filter $P_0(z) = H_0(z)F_0(z)$. In the general M-band case, it has been proven

TABLE I
DESIGN EXAMPLE 1: COEFFICIENTS OF THE 4-CHANNEL 8-TAP DYADIC LPPRFB. TOP: ANALYSIS FILTERS h_i. BOTTOM: SYNTHESIS FILTERS f_i

h_0	-5/16	1/8	7/8	21/16	21/16	7/8	1/8	-5/16
h_1	-61/512	9/256	95/256	141/512	-141/512	-95/256	-9/256	61/512
h_2	-1/8	0	1/2	-3/8	-3/8	1/2	0	-1/8
h_3	23/128	5/64	-61/64	249/128	-249/128	61/64	-5/64	-23/128
f_0	0	1/16	3/16	1/4	1/4	3/16	1/16	0
f_1	5/128	-23/256	-249/256	-61/128	61/128	249/256	23/256	-5/128
f_2	-1/16	-5/32	21/32	-7/16	-7/16	21/32	-5/32	-1/16
f_3	-9/512	-61/1024	141/1024	-95/512	95/512	-141/1024	61/1024	9/512

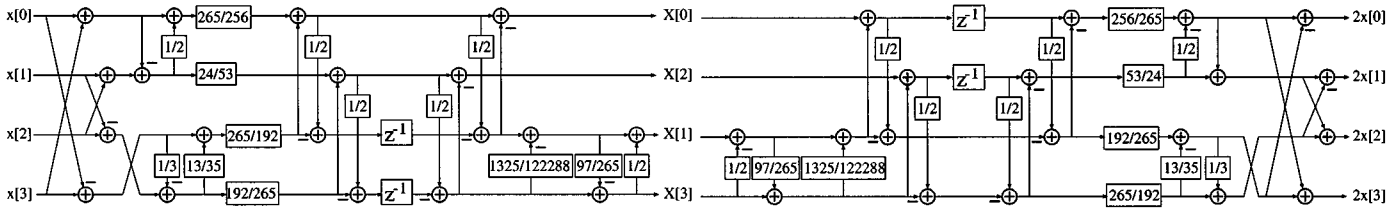

Fig. 11. Design Example 2: 4-channel 8-tap rational-coefficient LPPRFB with 1 analysis vanishing moment and 2 synthesis vanishing moments. Left: analysis bank. Right: synthesis bank.

that in order for $F_0(z)$ to be K-regular (having K zeros at $(2k\pi/M), \forall k = 1, 2, \ldots, M-1$), all $H_i(z), i = 1, 2, \ldots, M-1$, must have K zeros at dc frequency ($\omega = 0$) and vice versa [25]. The latter statement is equivalent to

$$\sum_{n=0}^{L-1} n^k h_i[n] = 0 \qquad \forall i = 1, 2, \ldots, M-1 \text{ and } \forall k = 0, 1, \ldots, K-1. \quad (11)$$

Taking advantage of the result in (11), we can enforce as many as K vanishing moments on the lowpass filter by designing the lifting steps in $\mathbf{U}_0$ and $\mathbf{V}_i$ such that the resulting lattice yields zero output in every subband except the lowpass one when it is excited with the set of input signals $\{n^k; k = 0, 1, \ldots, K-1\}$. A subset of lattice parameters $\{p_{ij}, u_{ij}\}$ will be allocated specifically for the imposition of vanishing moments, further reducing the number of free parameters in the lattice.

C. Design Example 1: 4-Channel 8-Tap Dyadic-Coefficient

In this 4-channel 8-tap design example, we demonstrate the feasibility of designing nontrivial integer-coefficient LPPRFBs. This design is obtained from the optimization approach based on the Type-I lattice. Floating-point lifting coefficients are first found via the nonlinear unconstrained optimization *simplex* routine in Matlab. Integer-coefficient solution is then obtained by quantizing the lifting coefficients to dyadic rationals. The corresponding fast implementation is depicted in Fig. 9. All of the filter coefficients are indeed dyadic, and they are tabulated in Table I. Note that the scaling factors 2 and 1/2 are present to balance the gain of the subbands only; they should be absorbed into the quantizer or moved to the other bank in practice. The normalized frequency responses of the filters are shown in Fig. 10.

D. Design Example 2: 4-Channel 8-Tap Rational-Coefficient With Improved Regularity

This 4-channel 8-tap design example has rational coefficients, instead of dyadic as in the previous one. It is still based on the Type-I lattice in Fig. 4(a). However, it was designed to have exactly one vanishing moment in the analysis bank and two vanishing moments in the synthesis bank. The synthesis stage can reconstruct perfectly the ramp signal using only the low-pass subband. The enhanced smoothness in the synthesis bank is evident from the scaling and the wavelet functions shown in Fig. 12. This design achieves the highest degree of regularity given the number of channels and the number of filter taps – it is impossible to impose two vanishing moments on the analysis bank as well [25]. The detailed lattice structure is depicted in Fig. 11. Unfortunately, this FB does not have a practical integer implementation due to the excessive dynamic range of the lifting parameters.

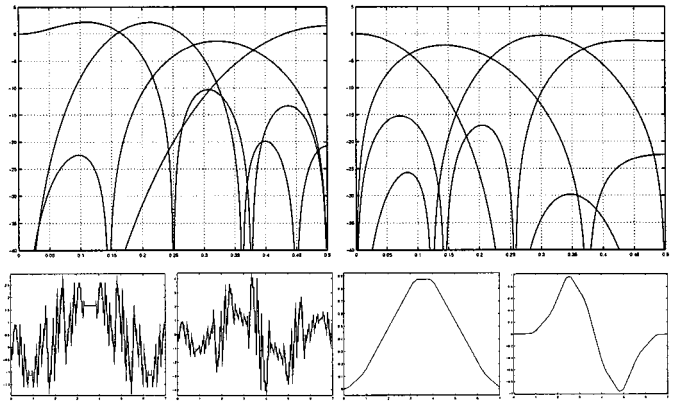

Fig. 12. Design Example 2. Top row: normalized frequency responses of the 4-channel 8-tap regular rational-coefficient LPPRFB (left: analysis; right: synthesis). Bottom row, from left to right: analysis scaling function $\phi^a(t)$, first analysis wavelet function $\psi_1^a(t)$, synthesis scaling function $\phi^s(t)$, and first synthesis wavelet function $\psi_1^s(t)$.

E. Design Example 3: 8-Channel 8-Tap Dyadic-Coefficient

This 8-channel 8-tap dyadic-coefficient design example is a close approximation of the 8×8 floating-point DCT [34]. Hence, it is named the binDCT and it follows the DCT's factorization very closely. The resulting multiplierless lattice structure

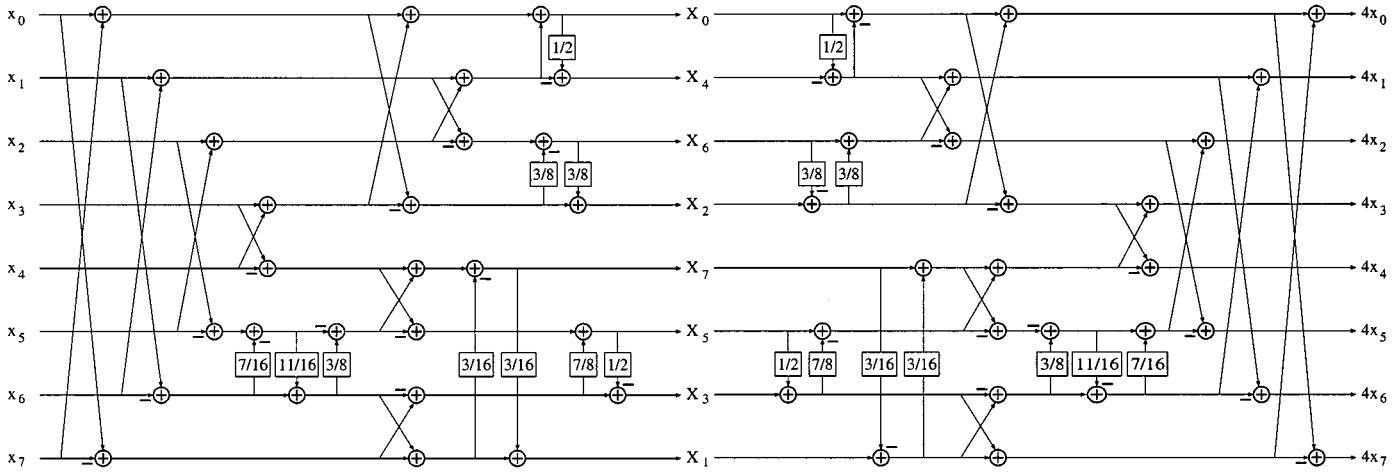

Fig. 13. Design example 3: 8-channel 8-tap binDCT. Left: analysis bank. Right: synthesis bank.

TABLE II
DESIGN EXAMPLE 3: COEFFICIENTS OF THE 8-CHANNEL 8-TAP DYADIC-COEFFICIENT LPPRFB. TOP: ANALYSIS FILTERS h_i. BOTTOM: SYNTHESIS FILTERS f_i

h_0	1/2	1/2	1/2	1/2	1/2	1/2	1/2	1/2
h_1	247/512	52811/131072	2147/8192	3/32	-3/32	-2147/8192	-52811/131072	-247/512
h_2	55/128	3/16	-3/16	-55/128	-55/128	-3/16	3/16	55/128
h_3	9/32	-89/4096	-97/256	-1/4	1/4	97/256	89/4096	-9/32
h_4	1/4	-1/4	-1/4	1/4	1/4	-1/4	-1/4	1/4
h_5	7/16	-1343/2048	9/128	1/2	-1/2	-9/128	1343/2048	-7/16
h_6	-3/16	1/2	-1/2	3/16	3/16	-1/2	1/2	-3/16
h_7	-3/32	2329/8192	-223/512	1/2	-1/2	223/512	-2329/8192	3/32
f_0	1/4	1/4	1/4	1/4	1/4	1/4	1/4	1/4
f_1	-1/2	-223/512	-2329/8192	-3/32	3/32	2329/8192	223/512	1/2
f_2	1/2	3/16	-3/16	-1/2	-1/2	-3/16	3/16	1/2
f_3	-1/2	9/128	1343/2048	7/16	-7/16	-1343/2048	-9/128	1/2
f_4	1/2	-1/2	-1/2	1/2	1/2	-1/2	-1/2	1/2
f_5	-1/4	97/256	-89/4096	-9/32	9/32	89/4096	-97/256	1/4
f_6	-3/16	55/128	-55/128	3/16	3/16	-55/128	55/128	-3/16
f_7	3/32	-2147/8192	52811/131072	-247/512	247/512	-52811/131072	2147/8192	-3/32

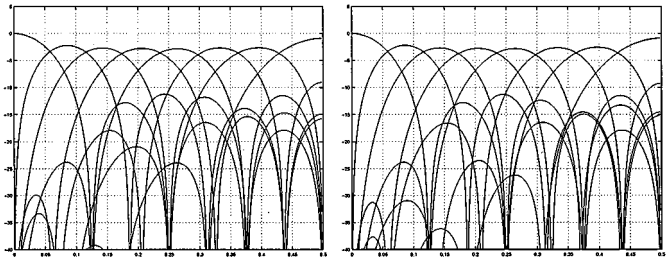

Fig. 14. Frequency responses of the 8-channel 8-tap binDCT in Design Example 3. Left: analysis bank. Right: synthesis bank.

is depicted in Fig. 13. Design Example 3 is obtained from the approximation approach. Each rotation angle in the Chen's DCT structure is converted to a lifting representation. We employ two lifting steps for the rotation angles near the output and three lifting steps for the single rotation angle in the middle of the structure. The scaling factors associated with the 2-lifting-step structure are combined with the quantization step sizes to save computational complexity further. The 8×8 binDCT's dyadic transform coefficients are listed in Table II. Its frequency responses are presented in Fig. 14. For more details on DCT approximation, we refer the readers to [36].

F. Design Example 4: 8-Channel 16-Tap LiftLT

This 8-channel 16-tap design example mimics the LOT [18] and the LBT [38] closely. However, the overlapping post-processing module is constructed solely using lifting steps; hence, we name the transform the LiftLT. In the 8×16 Type-I fast LOT, the three rotation angles that yield near-optimal solution are $\{0.13\pi, 0.16\pi, 0.13\pi\}$ [18]. It turns out that each of these rotation angles can be loosely approximated by a cascade of two 1/2 lifting steps. In other words, from the Type-I lattice in Fig. 4(a), the LiftLT has $\mathbf{U}_0$ and $\mathbf{V}_0$ chosen from the DCT whereas $\mathbf{V}_1 = \mathbf{L}_1\mathbf{L}_2 \ldots \mathbf{L}_{(M/2)-1}$, where

$$\mathbf{L}_i = \begin{bmatrix} \mathbf{I}_{M/2-i-1} & & \\ & \mathbf{L} & \\ & & \mathbf{I}_{i-1} \end{bmatrix}$$

with $\mathbf{L} = \begin{bmatrix} 1 & -1/2 \\ 0 & 1 \end{bmatrix} \begin{bmatrix} 1 & 0 \\ 1/2 & 1 \end{bmatrix}$. This solution yields a large

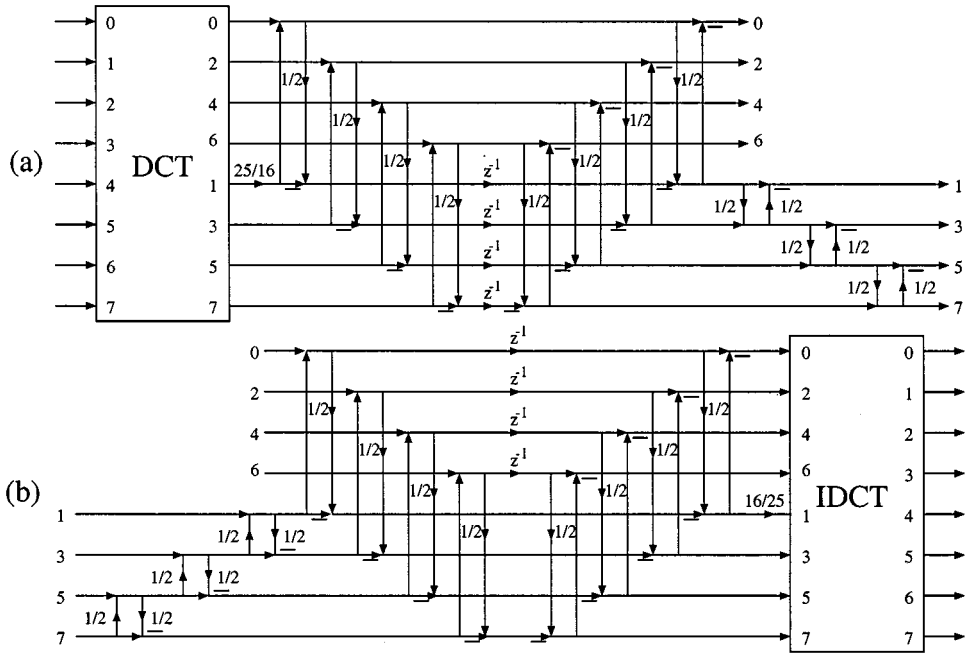

Fig. 15. Fast implementation of the 8-channel 16-tap LiftLT. (a) Analysis bank. (b) Synthesis bank.

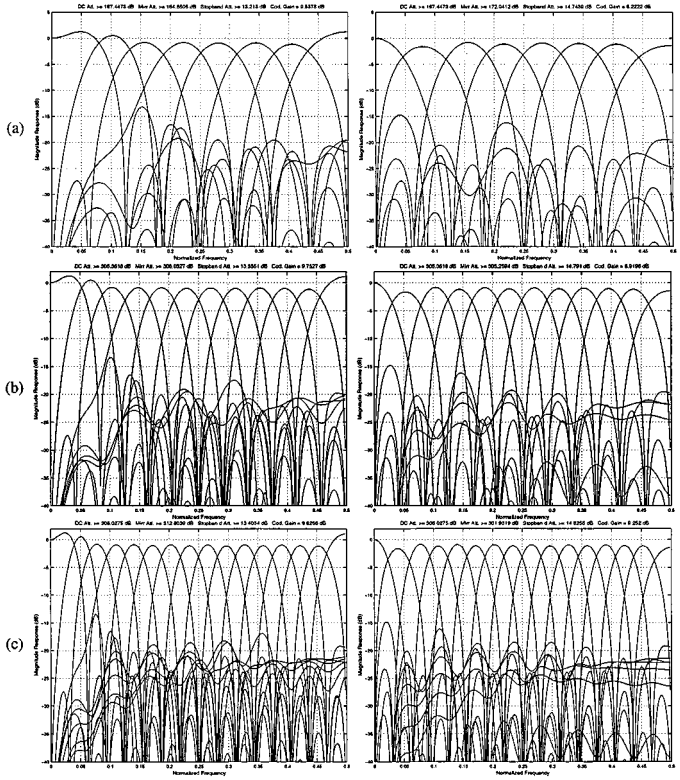

Fig. 16. Frequency responses of various LiftLT's. Left: analysis bank. Right: synthesis bank. (a) 8-channel 16-tap; 9.54 dB coding gain (b) 12-channel 24-tap; 9.75 dB coding gain. (c) 16-channel 32-tap; 9.83 dB coding gain.

class of even-channel LTs with 50% overlap ($L = 2M$). The 8-band LiftLT's lattice structure is presented in Fig. 15. The frequency responses of the 8×16, 12×24, and 32×64 LiftLT filters are depicted in Fig. 16. The reader should note that the LiftLT does not really have rational coefficients. It does have a dyadic post-filtering inter-block stage of DCT coefficients to improve coding efficiency. To obtain rational- or dyadic-coefficient LiftLT, we need to replace the DCT by a rational or dyadic approximation such as a binDCT version similar to design Example 3.

G. Design Example 5: 8-Channel 16-Tap Dyadic-Coefficient

This 8-band 16-tap dyadic-coefficient design example is obtained from the unconstrained optimization approach based on the Type-II lattice as in Fig. 4(b). Matrices $\mathbf{U}_0$ and $\mathbf{V}_0$ are parameterized in full, i.e., using 12 dyadic lifting steps for each, while $\mathbf{V}_1$ is parameterized with only six dyadic lifting steps. All diagonal scaling factors α_i are set to unity. The result not only has dyadic coefficients as illustrated in Table III, but it is also entirely lifting-based, has an efficient multiplierless implementation and maps integers to integers with perfect inversion as shown in Fig. 17. The normalized frequency responses of the filters are depicted in Fig. 18.

V. Image Coding Application

A. Computational Complexity and Coding Performance

This section provides a comparison of the computational complexity and the theoretical coding performance between the new rational or integer FBs and current state-of-the-art transforms. The five transforms in comparison are as follows:

- DCT: 8-channel 8-tap irrational-coefficient filters [34];
- Wavelet: 9/7-tap biorthogonal irrational-coefficient filters [39];
- binDCT: 8-channel 8-tap dyadic-coefficient filters (Design Example 3);
- LiftLT-I: 8-channel 16-tap irrational-coefficient filters (Design Example 4);
- LiftLT-II: 8-channel 16-tap dyadic-coefficient filters (Design Example 5).

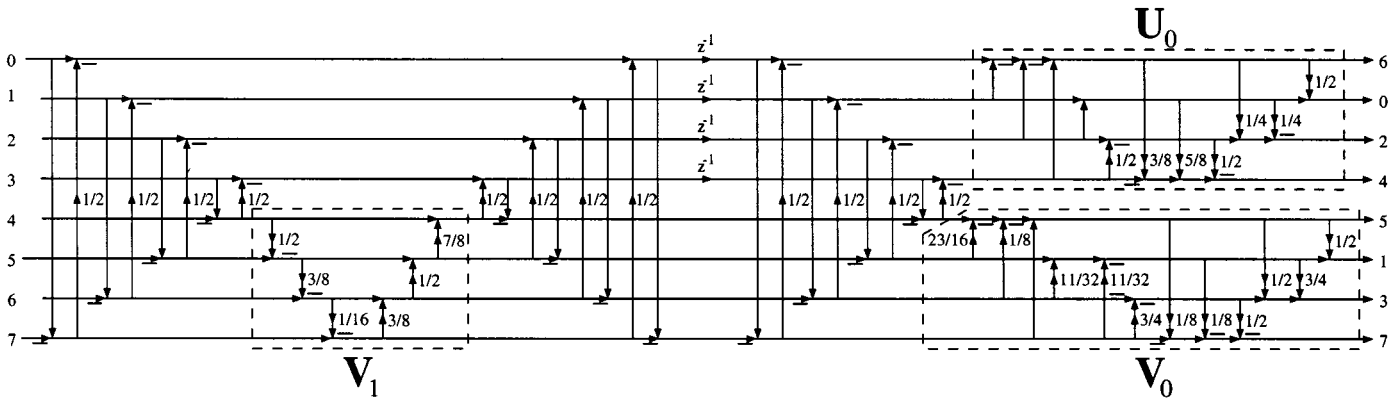

Fig. 17. Design example 5: 8-channel 16-tap LiftLT type-II.

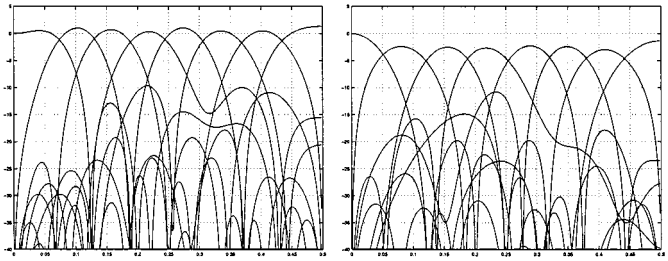

Fig. 18. Normalized frequency responses of the 8-channel 16-tap LiftLT-II in design example 5. Left: analysis bank. Right: synthesis bank.

TABLE III
DESIGN EXAMPLE 5: COEFFICIENTS OF 8-CHANNEL 16-TAP LPPRFB. TOP: ANALYSIS FILTERS h_i. BOTTOM: SYNTHESIS FILTERS f_i. EVEN-INDEXED FILTERS ARE SYMMETRIC WHEREAS ODD-INDEXED FILTERS ARE ANTI-SYMMETRIC

h_0	$-93/2^{10}$	$-1699/2^{14}$	$-3095/2^{17}$	$19479/2^{18}$	$46057/2^{18}$	$35863/2^{17}$	$5795/2^{14}$	$349/2^{10}$	...
h_1	$123/2^{10}$	$2741/2^{14}$	$13537/2^{17}$	$-31969/2^{18}$	$-99103/2^{18}$	$-50401/2^{17}$	$-7349/2^{14}$	$-283/2^{10}$	...
h_2	$15/2^{12}$	$5105/2^{16}$	$39981/2^{19}$	$-72749/2^{20}$	$-123859/2^{20}$	$-105517/2^{19}$	$3087/2^{16}$	$753/2^{12}$	...
h_3	$-219/2^{11}$	$4579/2^{15}$	$83159/2^{18}$	$-87255/2^{19}$	$-174889/2^{19}$	$-91351/2^{18}$	$21789/2^{15}$	$1259/2^{11}$	...
h_4	$51/2^{9}$	$205/2^{13}$	$-21095/2^{16}$	$4711/2^{17}$	$60825/2^{17}$	$-11673/2^{16}$	$-4301/2^{13}$	$205/2^{9}$	...
h_5	$-39/2^{9}$	$-1369/2^{13}$	$34315/2^{16}$	$12789/2^{17}$	$-143861/2^{17}$	$59893/2^{16}$	$2393/2^{13}$	$-473/2^{9}$	...
h_6	$69/2^{11}$	$-1093/2^{15}$	$5327/2^{18}$	$27441/2^{19}$	$-92977/2^{19}$	$60209/2^{18}$	$-7099/2^{15}$	$187/2^{11}$	...
h_7	$33/2^{9}$	$-79/2^{11}$	$-223/2^{14}$	$2719/2^{15}$	$-6815/2^{15}$	$5215/2^{14}$	$-825/2^{11}$	$201/2^{9}$	...
f_0	$-5/2^{9}$	$3/2^{6}$	$7/2^{6}$	$7/2^{5}$	$9/2^{5}$	$25/2^{6}$	$29/2^{6}$	$261/2^{9}$	...
f_1	$-15/2^{11}$	$-555/2^{14}$	$1967/2^{16}$	$3199/2^{14}$	$365/2^{10}$	$27281/2^{16}$	$5163/2^{14}$	$271/2^{11}$	...
f_2	$-1/2^{8}$	$21/2^{6}$	$17/2^{6}$	$-7/2^{5}$	$-25/2^{5}$	$-49/2^{6}$	$11/2^{6}$	$257/2^{8}$	...
f_3	$7/2^{10}$	$-657/2^{13}$	$-4387/2^{15}$	$77/2^{13}$	$119/2^{9}$	$5091/2^{15}$	$-1903/2^{13}$	$-263/2^{10}$	...
f_4	$11/2^{10}$	$9/2^{7}$	$-23/2^{7}$	$-7/2^{6}$	$23/2^{6}$	$-9/2^{7}$	$-41/2^{7}$	$245/2^{10}$	...
f_5	$5/2^{11}$	$949/2^{14}$	$-4783/2^{16}$	$-1407/2^{14}$	$179/2^{10}$	$-8081/2^{16}$	$-1451/2^{14}$	$251/2^{11}$	...
f_6	$15/2^{9}$	$-15/2^{7}$	$13/2^{7}$	$21/2^{6}$	$-53/2^{6}$	$83/2^{7}$	$-81/2^{7}$	$241/2^{9}$	...
f_7	$-9/2^{9}$	$-9/2^{12}$	$-11/2^{14}$	$-539/2^{12}$	$63/2^{8}$	$-4917/2^{14}$	$1545/2^{12}$	$-247/2^{9}$	...

TABLE IV
COMPARISON OF TRANSFORM COMPLEXITY AND THEORETICAL CODING GAIN

Transform	*No. of Multiplications*	*No. of Additions*	*No. of Shifts*	*Coding Gain*
9/7 Wavelet	5.25	7	0	9.46 dB
8×8 DCT	1.625	3.625	0	8.83 dB
8×8 binDCT	0	3.75	1.5	8.82 dB
8×16 LiftLT-I	1.75	6.375	0.75	9.54 dB
8×16 LiftLT-II	0	8.125	5.625	9.27 dB

Table IV tabulates the average number of multiplications, additions, and/or shifting operations needed to process one input sample in 1D, and the theoretical coding gain of each transform given an AR (1) signal model with intersample autocorrelation coefficient $\rho = 0.95$. The numbers associated with the 9/7-tap wavelet [39] are obtained from a 3-level decomposition implemented in the lifting scheme.

The evidence in Table IV shows that high-performance, yet low-complexity, FBs can be constructed based on our proposed lattice structures. Many of our design examples are faster than the 9/7-tap wavelet transform, even in its lifting implementation. The LiftLT-I in Design Example 4 and LiftLT-II in Design Example 5 are slower than the DCT; however, they eliminate blocking artifacts at a reasonable computational overhead, much

TABLE V
OBJECTIVE CODING RESULT COMPARISON (PSNR IN DB)

	Goldhill					*Barbara*				
Comp. Ratio	9/7 WL	8×8 DCT	8×8 binDCT	8×16 LiftLT-I	8×16 LiftLT-II	9/7 WL	8×8 DCT	8×8 binDCT	8×16 LiftLT-I	8×16 LiftLT-II
1:8	36.55	36.25	36.24	36.56	36.38	36.41	36.31	36.20	37.57	36.87
1:16	33.13	32.76	32.75	33.22	33.11	31.40	31.11	31.05	32.82	32.21
1:32	30.56	30.07	30.07	30.63	30.61	27.58	27.28	27.25	28.93	28.49
1:64	28.48	27.93	27.93	28.54	28.46	24.86	24.58	24.57	25.93	25.64

Fig. 19. Enlarged 256×256 Barbara portions at 32:1 compression ratio. Top row, from left to right: original image; coded by 9/7-tap wavelet, 27.58 dB; coded by 8×8 DCT, 27.28 dB. Bottom row, from left to right: coded by 8×8 binDCT, 27.25 dB; coded by 8×16 LiftLT-I, 28.93 dB; coded by 8×16 LiftLT-II, 28.49 dB.

less than 100%. The LiftLT-II does not even require any multiplication. Performance-wise, The LiftLT-I attains a coding gain very close to the 9.63 dB level of the optimal GLBT [21]. The improvement in coding performance over the DCT and sometimes the 9/7-tap wavelet transform is very promising as demonstrated by the image coding experiment in the next section.

B. Image Coding Experiment

The same SPIHT's quantizer and entropy coder [40] are utilized to encode the coefficients of every transform. The encoding algorithm is fixed; we only change the decomposition and the corresponding reconstruction stage. The transforms in the coding experiment are the same five compared in the last section. The test images are *Goldhill* and *Barbara*, both standard 512×512 8-bit grayscale images. The results obtained with the 9/7-tap wavelet (6 levels of decomposition here) are exactly those from the original SPIHT algorithm [40] . In the four 8-channel cases, we use the modified zerotree structure in [28], [41] where each block of transform coefficients are treated analogously to a full wavelet tree and three more levels of wavelet decomposition are employed to decorrelate the dc subband further. The objective coding results (PSNR in dB) are tabulated in Table V.

The LiftLT-I outperforms all transforms on both test images at all bit rates. The visual quality of its reconstructed images is also superior as testified in Fig. 19: blocking is completely avoided whereas ringing is reasonably contained. Comparing to the wavelet transform, the LiftLT-I consistently surpasses the 9/7-tap wavelet. The PSNR improvement can sometimes reach as high as 1.5 dB. Comparing to the LiftLT-I, the multiplierless

LiftLT-II sacrifices roughly a 0.5 dB loss on *Barbara* and a 0.1 dB loss on the smoother image *Goldhill*. Its performances are still very close to those of the 9/7-tap wavelet. The multiplierless binDCT yields roughly the same coding performances as the DCT.

VI. Summary

We have presented in this paper the theory, design, and implementation of M-channel LPPRFB with rational and dyadic coefficients. All new FBs are based on fast, efficient, robust, and modular lattice structures. Particularly, we have illustrated that rational-coefficient FBs can be easily designed by cascading rational lifting steps. Several low-complexity design examples are presented. All are fast-computable, VLSI-friendly, and hence can be valuable in fast real-time or low-cost, low-power signal processing applications. Two of our design examples, the 8-band 8-tap binDCT and the 8-band 16-tap LiftLT-II, can be implemented entirely using only shift-and-add binary operations. Furthermore, both can map integers to integers with exact reconstruction. This property allows a unifying lossy/lossless coding framework. Finally, the same design method can be easily extended to design fast and efficient FBs with longer filters, without linear-phase constraints, with an odd number of channels, or even with complex rational coefficients [42].

Acknowledgment

The authors wish to thank the anonymous reviewers for providing many constructive suggestions which significantly improve the presentation of the paper.

References

[1] P. P. Vaidyanathan, *Multirate Systems and Filter Banks*. Englewood Cliffs, NJ: Prentice-Hall, 1993.

[2] M. Vetterli and J. Kovačević, *Wavelets and Subband Coding*. Englewood Cliffs, NJ: Prentice-Hall, 1995.

[3] G. Strang and T. Q. Nguyen, *Wavelets and Filter Banks*. Wellesley, U.K.: Cambridge Univ. Press, 1996.

[4] C. S. Burrus, R. A. Gopinath, and H. Guo, *Introduction to Wavelets and Wavelet Transforms: A Primer*. Upper Saddle River, NJ: Prentice-Hall, 1998.

[5] D. LeGall and A. Tabatabai, "Subband coding of images using symmetric short kernel filters and arithmetic coding techniques," in *Proc. ICASSP*, 1988, pp. 761–764.

[6] B. R. Horng, H. Samueli, and A. N. Willson, "The design of low-complexity linear-phase FIR filter banks using power-of-two coefficients with an application to subband image coding," *IEEE Trans. Circuits Syst. Video Technol.*, vol. 1, pp. 318–323, Dec. 1991.

[7] A. A. M. L. Bruekens and A. W. M. van den Enden, "New networks for perfect inversion and perfect reconstruction," *IEEE J. Select. Areas Commun.*, vol. 10, pp. 130–137, Jan. 1992.

[8] A. N. Akansu, "Multiplierless PR quadrature mirror filters for subband image coding," *IEEE Trans. Image Processing*, vol. 5, pp. 1359–1363, Sept. 1996.

[9] R. C. Calderbank, I. Daubechies, W. Sweldens, and B. L. Yeo, "Wavelet transforms that map integers to integers," *Appl. Comput. Harmonic Anal.*, vol. 5, pp. 332–369, 1998.

[10] I. Daubechies and W. Sweldens, "Factoring wavelet transforms into lifting steps," *J. Fourier Anal. Appl.*, vol. 4, pp. 247–269, 1998.

[11] D. Wei, J. Tian, R. O. Wells Jr, and C. S. Burrus, "A new class of biorthogonal wavelet systems for image transform coding," *IEEE Trans. Image Processing*, vol. 7, pp. 1000–1013, July 1998.

[12] H. Y. Jung and R. Prost, "Lossless subband coding system based on rounding transform," *IEEE Trans. Signal Processing*, vol. 46, pp. 2535–2540, Sep. 1998.

[13] W. B. Pennebaker and J. L. Mitchell, *JPEG: Still Image Compression Standard*. New York: Van Nostrand Reinhold, 1993.

[14] J. L. Mitchell, D. LeGall, and C. Fogg, *MPEG Video Compression Standard*. New York: Chapman & Hall, 1996.

[15] D. Taubman, "High performance scalable image compression with EBCOT," *IEEE Trans. Image Processing*, vol. 9, pp. 1158–1170, Jul. 2000.

[16] ——, "JPEG2000 Verification Model: Version VM3A," IEC, Geneva, Switzerland, ISO/IEC JTC 1/SC 29/WG1 N1143, 1999.

[17] A. K. Soman, P. P. Vaidyanathan, and T. Q. Nguyen, "Linear-phase paraunitary filter banks: theory, factorizations and applications," *IEEE Trans. Signal Processing*, vol. 41, pp. 3480–3496, Dec. 1993.

[18] H. S. Malvar, *Signal Processing with Lapped Transforms*. Norwood, MA: Artech House, 1992.

[19] R. L. de Queiroz, T. Q. Nguyen, and K. R. Rao, "The GenLOT: generalized linear-phase lapped orthogonal transform," *IEEE Trans. Signal Processing*, vol. 40, pp. 497–507, Mar. 1996.

[20] M. Vetterli and D. Le Gall, "Perfect-reconstruction filter banks : some properties and factorizations," *IEEE Trans. Acoust., Speech, Signal Processing*, vol. 37, pp. 1057–1071, July 1989.

[21] T. D. Tran, R. L. de Queiroz, and T. Q. Nguyen, "Linear phase perfect reconstruction filter bank: lattice structure, design, and application in image coding," *IEEE Trans. Signal Processing*, vol. 48, pp. 133–147, Jan. 2000.

[22] X. Q. Gao, T. Q. Nguyen, and G. Strang, "On factorization of M-channel paraunitary filter banks," *IEEE Trans. Signal Processing*, vol. 49, pp. 1433–1446, July 2001.

[23] L. Gan and K. K. Ma, "A simplified lattice factorization for linear-phase perfect reconstruction filter bank," *IEEE Signal Processing Lett.*, vol. 8, pp. 207–209, July 2001.

[24] J. N. Bradley, C. M. Brislawn, and T. Hopper, "The FBI wavelet/scalar quantization standard for gray-scale fingerprint image compression," in *Proc. VCIP*, Orlando, FL, Apr. 1993.

[25] P. Steffen, P. N. Heller, R. A. Gopinath, and C. S. Burrus, "Theory of regular M-band wavelets," *IEEE Trans. Signal Processing*, vol. 41, pp. 3497–3511, Dec. 1993.

[26] R. Coifmann, Y. S. Q. Meyer, and M. V. Wickerhauser, *Signal Processing With Wavelet Packets*. New Haven, CT: Yale Univ., Numerical Algorithm Research Group, 1990.

[27] M. V. Wickerhauser, *Adapted Wavelet Analysis from Theory to Software*. Wellesley, MA: A.K. Peters, 1995.

[28] T. D. Tran and T. Q. Nguyen, "A progressive transmission image coder using linear-phase uniform filter banks as block transforms," *IEEE Trans. Image Processing*, vol. 8, pp. 1493–1507, Nov. 1999.

[29] D. Rauschmayer, *ADSL/VDSL Principles: A Practical and Precise Study of Asymmetric Digital Subscriber Lines and Very High Speed Digital Subscriber Lines*. New York: Macmillan, 1998.

[30] X.-G. Xia, "New precoding for intersymbol interference cancellation using nonmaximally decimated multirate filterbanks with ideal FIR equalizers," *IEEE Trans. Signal Processing*, vol. 45, pp. 2431–2440, Oct. 1997.

[31] A. Scaglione, G. B. Giannakis, and S. Barbarossa, "Redundant filterbank precoders and equalizers – Part I: unification and optimal design," *IEEE Trans. Signal Processing*, vol. 47, pp. 1988–2006, July 1999.

[32] R. A. Horn and C. R. Johnson, *Matrix Analysis*. Cambridge, U.K.: Cambridge Univ. Press, 1985.

[33] N. H. E. Weste and K. Eshragian, *Principles of CMOS VLSI Design: A System Perspective*, 2nd ed. New York: Addison-Wesley, 1993.

[34] K. R. Rao and P. Yip, *Discrete Cosine Transform: Algorithms, Advantages, Applications*. New York: Academic, 1990.

[35] J. Katto and Y. Yasuda, "Performance evaluation of subband coding and optimization of its filter coefficients," in *Proc. SPIE Visual Communication and Image Processing*, Boston, MA, Nov. 1991, pp. 95–106.

[36] T. D. Tran, "The BinDCT: fast multiplierless approximation of the DCT," *IEEE Signal Processing Lett.*, vol. 7, pp. 145–149, June 2000.

[37] J. Liang and T. D. Tran, "Fast multiplierless approximations of the DCT with the lifting scheme," *IEEE Trans. Signal Processing*, vol. 49, pp. 3032–3044, Dec. 2001.

[38] H. S. Malvar, "Biorthogonal and nonuniform lapped transforms for transform coding with reduced blocking and ringing artifacts," *IEEE Trans. Signal Processing*, vol. 46, pp. 1043–1053, Apr. 1998.
[39] M. Antonini, M. Barlaud, P. Mathieu, and I. Daubechies, "Image coding using wavelet transform," *IEEE Trans. Image Processing*, vol. 1, pp. 205–220, Apr. 1992.
[40] A. Said and W. A. Pearlman, "A new fast and efficient image codec based on set partitioning in hierarchical trees," *IEEE Trans. Circuits Syst. Video Technol.*, vol. 6, pp. 243–250, June 1996.
[41] H. S. Malvar, "Fast progressive image coding without wavelets," in *Proc. Data Compression Conf.*, Snowbird, Utah, Mar. 2000, pp. 243–252.
[42] S. Oraintara, Y.-J. Chen, and T. Q. Nguyen, "Integer fast Fourier transform," *IEEE Trans. Signal Processing*, vol. 50, pp. 607–618, Mar. 2002.

Trac D. Tran (S'94–M'98) received the B.S. and M.S. degrees from the Massachusetts Institute of Technology, Cambridge, in 1993 and 1994, respectively, and the Ph.D. degree from the University of Wisconsin, Madison, in 1998, all in electrical engineering.

He joined the Department of Electrical and Computer Engineering, The Johns Hopkins University, Baltimore, MD, in July 1998 as an Assistant Professor. His research interests are in the field of digital signal processing, particularly in multirate systems, filter banks, transforms, wavelets, and their applications in signal analysis, compression, processing, and communications. Dr. Tran was the co-director (with Prof. J. L. Prince) of the 33rd Annual Conference on Information Sciences and Systems (CISS'99), Baltimore, MD, in March 1999.

Dr. Tran received the NSF CAREER award in 2001.